JGR Oceans

RESEARCH ARTICLE
10.1029/2021JC017579

Spatial and Temporal Variability of the Gulf Stream Near Cape Hatteras

M. Andres[1]

[1]Woods Hole Oceanographic Institution, Woods Hole, MA, USA

Key Points:

- At Cape Hatteras, the nature of Gulf Stream position and transport variability changes over a 60-km distance from a red to a blue spectrum
- Wave-like Gulf Stream meanders decay approaching Cape Hatteras with temporal amplitude variability that may be driven by the Loop Current
- Florida Current transport maxima, coherent along the South Atlantic Bight, precede offshore Gulf Stream shifts downstream of Cape Hatteras

Correspondence to:
M. Andres,
mandres@whoi.edu

Citation:
Andres, M. (2021). Spatial and temporal variability of the Gulf Stream near Cape Hatteras. *Journal of Geophysical Research: Oceans*, *126*, e2021JC017579. https://doi.org/10.1029/2021JC017579

Received 25 MAY 2021
Accepted 11 AUG 2021

Abstract In situ observations from a 19-month deployment of current- and pressure-sensor equipped inverted echo sounders (CPIESs) along and across the Gulf Stream near Cape Hatteras capture spatial and temporal variability where this western boundary current separates from the continental margin. Regional hydrographic casts and two temperature cross-sections spanning the Gulf Stream southeast of Cape Hatteras are used with the CPIESs' records of acoustic travel time to infer changes in thermocline depth D_T and Gulf Stream position. Wave-like Gulf Stream meanders are observed where the Stream approaches the separation location with periods less than 15 days, wavelengths less than 500-km, and phase speeds between 40 and 70 km d^{-1}. Though meander amplitudes typically decrease by ~30% on the final approach to Cape Hatteras, some signals are still coherent across the Gulf Stream separation location. Temporal variability in meander intensity may be related to the Loop Current ~1,400 km upstream. Mesoscale variability is strongest downstream of the separation location where Gulf Stream position is no longer constrained by the steep continental slope. Low frequency transport changes in the Florida Straits are correlated with sea-surface height gradients along the entire South Atlantic Bight (SAB) and with D_T inferred at the CPIES sites. The correlations with D_T are likely due to coherent transport anomalies in the Gulf Stream approaching the separation location, which then drive Gulf Stream position changes downstream of the separation location. The patterns of coherent transport anomalies may reflect large-scale atmospheric forcing patterns or rapid equatorward propagation of barotropic signals along the SAB.

Plain Language Summary In the waters east of Cape Hatteras, many oceanographic processes co-occur within a small geographic footprint. Here northward-flowing waters on the South Atlantic Bight shelf collide with southward-flowing waters on the Middle Atlantic Bight shelf, resulting in complex exchanges that mingle waters from the shelves with one another and with open-ocean waters. These waters have distinct physical characteristics and since they experience different bio-geo-physical histories, they can also have distinct nutrient and sediment concentrations. Water-mass intermingling has far-reaching consequences for air-sea interactions, coupled biophysical processes, and geochemical balances. Just offshore is the Gulf Stream, a key component of the wind-driven system of swift surface currents and a limb of the heat pump by which the atmosphere and ocean work together to modulate earth's surface temperatures by moving heat from the equator pole-ward. Near the Cape, the Gulf Stream makes a major transition from a western boundary current flowing along the continental slope to a vigorously meandering jet. Gulf Stream variability plays an important role in controlling local cross-shelf exchange processes and is examined at scales from days to months using in situ observations from an array of current- and pressure-sensor equipped inverted echo sounders deployed for 19 months near the Cape.

1. Introduction

The Gulf Stream, the swift, surface-intensified current that carries warm, salty subtropical waters poleward through the Florida Straits and along the continental margin of the southeastern United States, separates from the margin near Cape Hatteras (Figure 1). Fed by net inflow along the seaward edge of the Stream, this western boundary current's mean transport changes downstream by almost a factor of three, increasing from 33 Sv in the Straits of Florida (Heiderich & Todd, 2020) to 88 Sv in the upper 2,000 m just beyond Cape Hatteras at 73°W (Halkin & Rossby, 1985).

Along its route, the absolute dynamic topography slopes across the Gulf Stream. On average, sea surface height (SSH) is more than 1 m higher on the Stream's seaward edge in the Sargasso Sea than on the

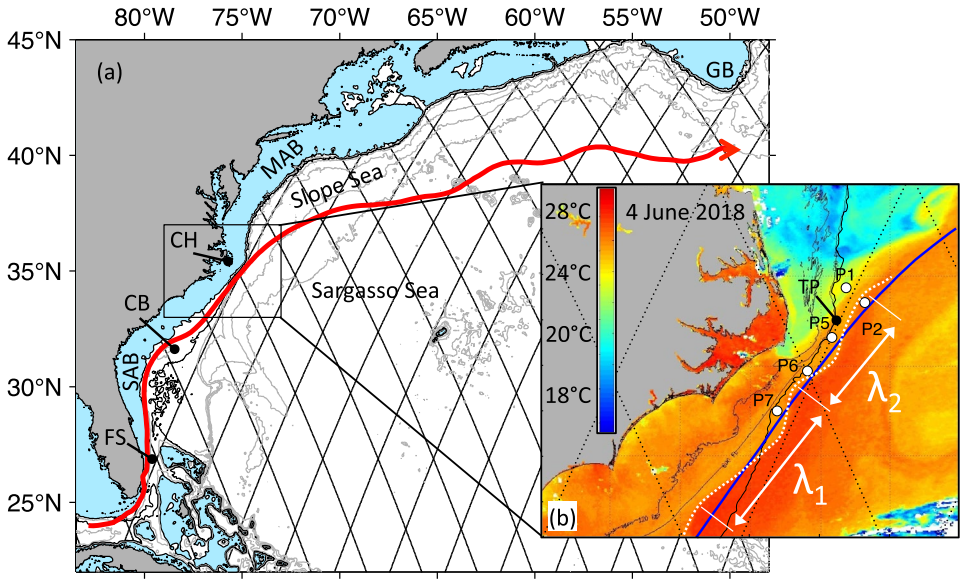

Figure 1. Panel (a): time-averaged (1993–2018) Gulf Stream path inferred from satellite altimetry using the 25.1-cm sea surface height (SSH) contour (red curve). Labels show Florida Straits (FS), South Atlantic Bight (SAB), Charleston Bump (CB), Cape Hatteras (CH), Middle Atlantic Bight (MAB), and Tail of the Grand Banks (GB). Waters on the shelves (shallower than 200-m) are shaded blue, and gray contours denote the 500–4500-m depths at 500-m intervals; the 800-m isobath (a stretch of which marks the offshore edge of the CB) is highlighted (black). The diamond pattern shows the Topex-Poseidon/Jason-1, 2, 3 repeat satellite tracks. Panel (b): snapshot of sea surface temperature (SST, from NOAA-15) off Cape Hatteras during a time with three meander crests (shoreward path excursions) clearly visible. CPIES locations are superimposed (white circles) and dashed white curve highlights a couple of meanders, which were propagating northeastward. The meander wavelengths show a decrease approaching CH (λ_1 is about 200 km and λ_2 is about 140 km). Satellite tracks are as in (a), as is the location of the Gulf Stream mean path (in this case shown in blue). The Point (TP), at 35.5°N, 74.8°W where the orientation of the 800-m isobath changes abruptly, is indicated.

shoreward edge. The Gulf Stream's maximum velocity core is collocated with the maximum in this cross-stream SSH gradient (e.g., Andres et al., 2020) and the surface geostrophic velocities in this limb of the North Atlantic subtropical gyre can exceed 2 m s^{-1} (Heiderich and Todd., 2020).

The path of the Gulf Stream velocity core varies at a range of spatial and temporal scales, and the nature of that variability is distinct up- and downstream of Cape Hatteras. From the Charleston Bump (~32°N) to Cape Hatteras, Gulf Stream path variability is dominated by wave-like meanders with amplitudes reaching about 40 km (Bane & Brooks, 1979). These decay on their approach to Cape Hatteras where the isobaths of the continental slope converge and the steepened bathymetric slope stabilizes the Stream's path (Gula et al., 2015; Lee et al., 1991; Savidge, 2004). Wavelike meanders, with dominant periods of 4–5 days, are superimposed on slower onshore/offshore shifts of the Gulf Stream path that persist for several months and may be triggered when cold core rings impinge on the Gulf Stream in the vicinity of Cape Hatteras (Bane & Dewar, 1988; Glenn & Ebbesmeyer, 1994).

Downstream of Cape Hatteras, the path of the separated Gulf Stream varies at seasonal scales, with a northward-shifted path (and relatively low transport) reportedly found in summer/fall and a southward-shifted path (and relatively high transport) observed in winter/spring (Tracey & Watts, 1986). In addition, downstream growth over a distance of about 375 km has been observed here for meanders at 4–5 day and 10–33 day periods (Tracey & Watts, 1986).

Further downstream, east of 70°W, the most striking variation in Gulf Stream path is the development of large-amplitude meander crests and troughs (e.g., Lee & Cornillon, 1996). These may remain stationary or move eastward slowly (up to 13.4 cm s^{-1} reported by Cornillon, 1986) relative to advection by the Gulf Stream, which is an order of magnitude faster.

While many studies have focused on Gulf Stream path variability on one side of Cape Hatteras or the other, the degree to which variability upstream of Cape Hatteras is coherent with that downstream of the Cape has also been investigated in a handful of studies. Savidge (2004) used 1-year records from instruments bracketing the separation location, which is the time-variable location where the Gulf Stream path changes from primarily along-isobath to cross-isobath as the current veers away from the upper slope and into the interior ocean. Observations from moorings embedded in the cyclonic-shear flank of the Gulf Stream suggest that path variance is concentrated at shorter periods (4–9 day period) just upstream of the separation location compared to that just downstream where the variance is primarily at ~45-day period (Savidge, 2004). At most frequencies, the Gulf Stream path variations captured by these records were not found to be significantly coherent over the 140-km downstream distance between the moorings spanning Cape Hatteras. Nevertheless, there is evidence that cold domes of cyclonically circulating upwelled water associated with meander troughs (i.e., offshore path excursions) approaching Cape Hatteras can be advected past Cape Hatteras and may persist downstream as identifiable features on the Stream's cyclonic flank (Glenn & Ebbesmeyer, 1994).

Variability in the Gulf Stream's path can influence along-shelf flow and cross-shelf exchange, both on the South Atlantic Bight (SAB) continental shelf south of Cape Hatteras (Miller and Lee, 1995a, 1995b) and on the Middle Atlantic Bight (MAB) shelf to the north (Bane et al., 1988). Adjacent to the SAB just south of Cape Hatteras, the cyclonic flank of the Gulf Stream is generally found over the 2000-m isobath. Gulf Stream velocities here are highly correlated with northeastward-directed (toward Cape Hatteras) flow over the 60-m isobath on the SAB outer-shelf (Savidge, 2004). Along the SAB, the wave-like Gulf Stream meanders (e.g., Figure 1b) induce cyclonic circulation in frontal eddies that are advected downstream between adjacent meander crests on the shoreward side of the Stream. These upwell cold, nutrient-rich waters and serve as a "nutrient pump" to the SAB shelf (Glenn & Ebbesmeyer, 1994; Gula et al., 2016; Lee et al., 1991).

Within the southern region of the MAB, where the Gulf Stream continues northeastward while the continental slope orientation changes rather abruptly from northeastward to northward at The Point, Gulf Stream influence on the shelf is more indirect. Here, the northeastward Gulf Stream flow becomes separated from the southward flow on the MAB outer shelf, with the Slope Sea in between, and the currents in the Gulf Stream cyclonic flank are poorly correlated with those over the 60-m isobath on the MAB outer-shelf (Savidge, 2004). However, Gulf Stream position here is correlated with along-shelf transport convergence near Cape Hatteras and, by inference, shelf export. Savidge and Bane (2001) report that an onshore-shifted Gulf Stream is positively correlated with stronger along-shelf transport convergence (and hence, stronger off-shelf transport), presumably due to Gulf Stream influence on the effectiveness of the various shelf-export mechanisms spanning the Hatteras Front, which is the oceanographic feature where the along-shelf flows of the equatorward MAB and poleward SAB shelf flows converge (Savidge & Austin, 2007).

To better understand these shelf-export mechanisms and the processes, which drive the net shelf export, an observational array was deployed near Cape Hatteras on the shelf and the neighboring continental slope areas spanning the typical range of the Hatteras Front location. These in situ time series measurements were supplemented by shipboard measurements (Andres et al., 2018; Han et al., 2021), glider missions (Todd, 2020a), and shore-based high-frequency (HF) radar observations (Haines et al., 2017). These observations and a hierarchy of numerical models comprise the National Science Foundation-funded PEACH (Processes driving Exchange At Cape Hatteras) research program. The PEACH observations also helped support the ongoing North Carolina Renewable Ocean Energy Program (NCROEP), with previous observations from NCROEP also complementing the PEACH Array (Muglia et al., 2020). Variability in the Gulf Stream, which serves as a shelf boundary condition and a potential driver of shelf export processes (e.g., Savidge & Bane, 2001), was measured in PEACH with bottom-moored current and pressure-sensor equipped inverted echo sounders (CPIESs, Figure 1b).

This paper reconsiders the Gulf Stream near Cape Hatteras using these new PEACH CPIES observations to (a) more completely characterize the scales of variability spanning the region where this current separates from the continental margin, and (b) examine the controls on and consequences of Gulf Stream variability near the Stream's separation location. Section 2 describes the CPIES measurements and several additional datasets that are used to provide context for the PEACH experiment. Section 3 explains the methods used to infer thermocline depth and Gulf Stream position from the CPIES records. Variability in signals spanning

Table 1
Processes Driving Exchange at Cape Hatteras (PEACH) Current- and Pressure-Sensor Equipped Inverted Echo Sounder (CPIES) Sites

Site ID	Latitude (°N)	Longitude (°W)	Water depth (m)	Spacing (km)
P1	35.8517	74.6167	1,776	-
P2	35.6894	74.3500	2,349	30
P5	35.3080	74.8202	1,798	60
P6	34.9400	75.1664	1,275	52
P7	34.5000	75.6000	1,313	63

Cape Hatteras is examined in Section 4, and Section 5 considers the variability observed with the PEACH Array off Cape Hatteras in the context of the upstream Gulf Stream and the broader western North Atlantic region. Section 6 summarizes the results and considers areas for future study.

2. Data

2.1. CPIESs and the Bottom-to-Surface Round-Trip Acoustic Travel Time

Five CPIESs were deployed as part of the PEACH Array from April 2017 through November 2018 in water depths ranging from 1,300 to 2,350 m (Table 1). These sites are onshore of the time-averaged path of the Gulf Stream velocity core (Figure 2) and are often within the cyclonic flank of the meandering Stream. Three of the sites are along the continental slope offshore of the SAB (from south to north: P7, P6, and P5) on the Gulf Stream's approach to The Point, which is where the 800-m isobath orientation turns sharply from northeastward to northward (Figure 1b). Two sites (P1 and P2) are east of the southern tip of the MAB shelf, and just downstream of the time-variable separation location where the Gulf Stream crosses isobaths as it leaves the continental margin. P2 is often within the meandering Gulf Stream, while P1 is generally onshore of this swift northeastward-flowing current. Spacing between neighboring PEACH CPIESs ranges from 30 to 63 km (Table 1).

Each CPIES was deployed on the seabed and recorded the hourly round-trip surface-to-bottom acoustic travel time τ from April 2017 through November 2018. The τ records are complete except for a short gap at P5 from June 6 to 14, 2017 (Figure 3). The CPIESs also recorded hourly bottom pressure P_B and temperature T_B, and near-bottom horizontal currents. The τ records are used here to infer thermocline depth in the Gulf Stream and to examine Gulf Stream variability at daily to monthly time scales. The pressure records are used to determine the instrument deployment depths from each instrument's time-mean P_B, with the mean atmospheric sea level pressure (10.13 dbar) removed (Table 1). Further analysis of the CPIESs' time-varying P_B, T_B, and near-bottom currents will be reported elsewhere.

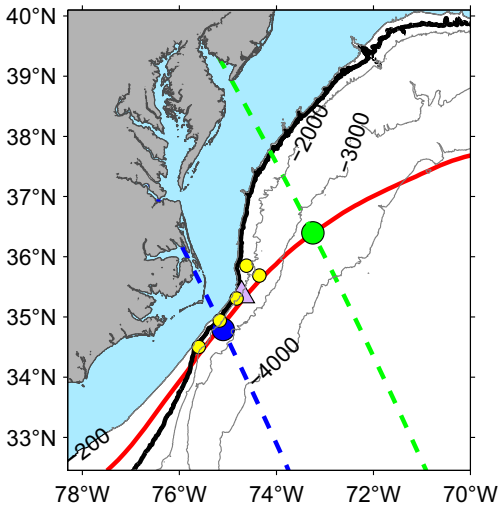

Figure 2. Bathymetry near Cape Hatteras from the GEBCO_2014 Grid, version 20150318 (http://www.gebco.net), with depths shallower than 200 m shaded (blue) and the 800-m isobath highlighted (heavy black). Also shown are satellite altimeter track-152 (blue dashed) and track-228 (green dashed) with the mean satellite-derived Gulf Stream core position (from |δSSH/δx|) on each track indicated by the filled circle. CPIES sites are shown with yellow dots. For reference, mooring B4 (purple triangle) reported on by Savidge (2004) and the Gulf Stream path inferred from the time-averaged 25.1-cm SSH contour (red, as in Figure 1) are shown.

Details of the τ processing are described in a technical report (Andres, 2020) and follow Kennelly et al. (2007). Briefly, the CPIESs' hourly τ measurements are 2-day low-pass filtered, providing records that resolve high-frequency processes associated with the region's ubiquitous Gulf Stream meanders in a 3–25-day band, as well as lower frequency processes. To compare variability across sites and to track signal propagations between sites, each 2-day low-pass filtered record is converted to a common reference level, in this case 950 dbar, giving τ_{950}, which is the travel time that would have been recorded at each site if the instruments were all deployed at the same depth.

2.2. Complementary Datasets

2.2.1. Along-Track Satellite Altimetry

Along-track satellite altimetry, which delivers high spatial resolution (~6 km) measurements of the ocean's absolute dynamic topography along repeated tracks for long duration (1993-present), is used here to provide spatial context about the position of the Gulf Stream across lines bracketing the PEACH CPIES sites. Where these tracks cross the Gulf Stream, the time-varying maximum in the along-track gradient of SSH (|δSSH/δx|) serves as a good proxy of position of the Gulf Stream velocity maximum. Along-track satellite data are available from Copernicus

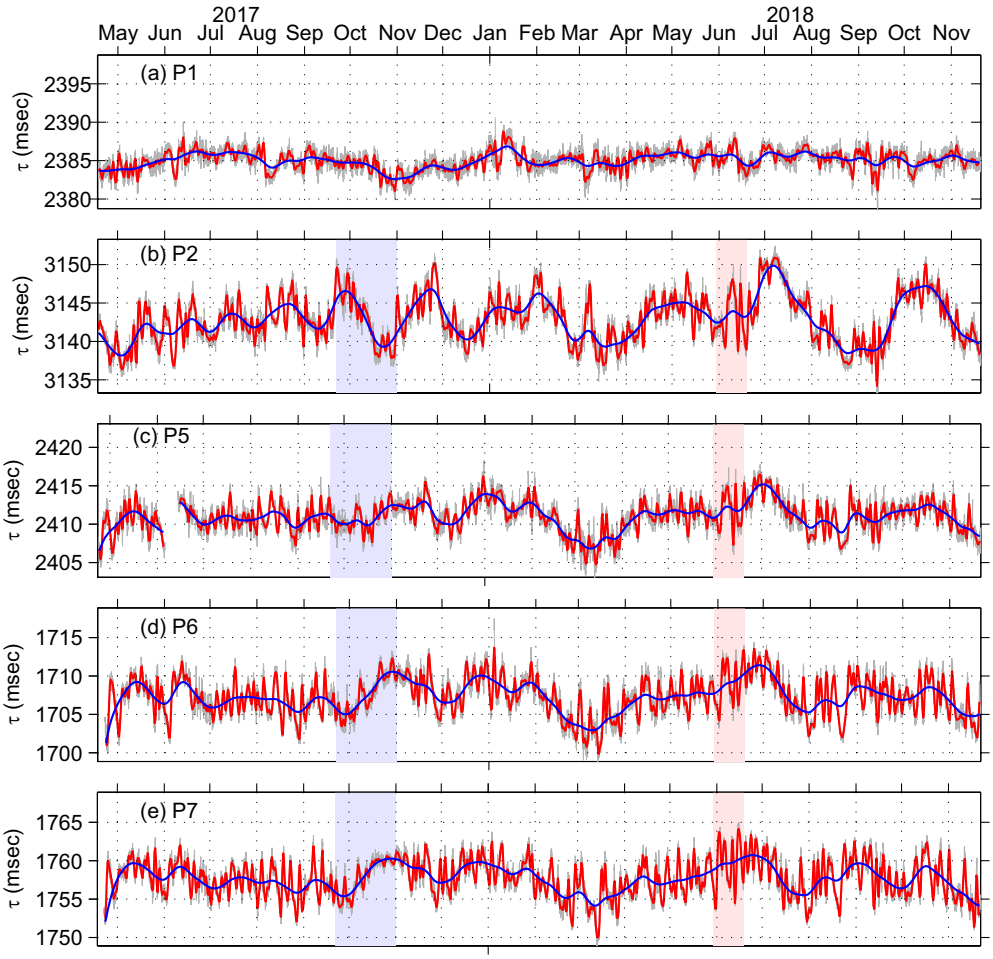

Figure 3. CPIES-measured τ records shown hourly (gray), 2-day low pass filtered (red), and 25-day low pass filtered (blue). Shading highlights periods with particularly low (blue) and high (pink) intensity of meander amplitudes in the 3–22-day band at sites P2 and P5–P7, discussed in Section 5.1.

Marine Service. The global ocean level-3 reprocessed SSH products (SEALEVEL_GLO_PHY_L3_REP_OBSERVATIONS_008_062) from two tracks that span Cape Hatteras are used for this study.

Satellite track-152 crosses the Gulf Stream as it flows northeastward, adjacent to the SAB shelf, about 60 km upstream of The Point (Figure 2). This track cuts across the 140-km long segment of the continental slope where the 100–3,000-m isobaths converge and the bathymetry is particularly steep. The neighboring satellite track to the northeast, track-228, crosses the Gulf Stream about 180 km downstream of The Point and beyond the time-varying separation location near Cape Hatteras were the current begins to diverge from the continental margin and flows across isobaths into deeper waters. For each track, the repeat measurement cycle is 9.9157 days. The measurements across the Gulf Stream from track-228 are made 2.9665 days after those from track-152.

2.2.2. Mapped Satellite Observations

Maps of SST from AVHRR (Advanced Very-High-Resolution Radiometer) and SSH from satellite altimeters provide broader spatial context for the PEACH CPIES measurements. SST is plagued by frequent cloud cover in the region near Cape Hatteras. For some applications, this can be mitigated by using multiday composite SST averages or reanalysis products. However, since these likely alias the wave-like meanders that rapidly propagate by Cape Hatteras, only a handful of "snapshots" that resolve the meanders (e.g., Figure 1b) are used here for a qualitative estimate of changes to Gulf Stream meanders as they approach

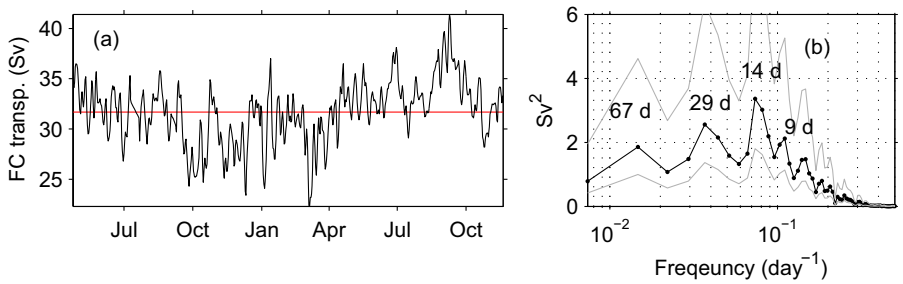

Figure 4. Panel (a): daily (black) and time-averaged (red) volume transport through the Florida Straits during the PEACH experiment period, inferred from a submarine cable. Panel (b): variance preserving spectrum of the Florida Current transport during this time interval (black curve), calculated with a 136-day window and 50% overlap. Gray lines indicate the 95% confidence limits.

and pass the Cape. SST images of the region are available from the Rutgers Coastal Ocean Observation lab (https://rucool.marine.rutgers.edu).

SSH maps at daily intervals and ¼° resolution are available from Copernicus Marine Service. The level-4 reprocessed observations (SEALEVEL_GLO_L4_REP_OBSERVATIONS_008_047) are used here to generate lagged-correlation maps and to identify the mean location of the Gulf Stream path along its entire route from a single SSH contour. For the latter, the 25-cm contour of absolute dynamic topography serves as an excellent proxy of the mean and time-varying Gulf Stream path downstream of Cape Hatteras (e.g., Andres, 2016; Lillibridge & Mariano, 2013). Comparisons with observations from upward-looking acoustic Doppler current profilers (ADCPs) moored along a satellite track confirm that the location of the 25-cm contour coincides with the maximum in the near-surface velocities of the Gulf Stream core (Andres et al., 2020). In the present work, however, which examines the Gulf Stream path over a larger domain, it is found that the time-mean 25.0 cm SSH contour intersects the coast of Florida, so the 25.1-cm SSH contour is used instead as a proxy for Gulf Stream path (e.g., Figure 1a, red curve). Heiderich and Todd (2020), who examine the Gulf Stream from Miami to New England, use the 40-cm contour. Temporal and spatial variations in the locations of these SSH contours between 25 and 40-cm contours are highly correlated with one another since they fall within the Gulf Stream core where the sea surface is steeply sloped and the currents are large (figure not shown). The results presented here are qualitatively the same, regardless of which contour is used.

2.2.3. Florida Current Transport

The strength of the Gulf Stream through Florida Straits, referred to as the Florida Current, has been monitored since 1986 using a submarine cable that crosses beneath the Gulf Stream at 26.5°N. The voltage difference, regularly calibrated with shipboard measurements, is used to infer the daily Florida Current volume transport (e.g., Meinen et al., 2010). The Florida Current data are made freely available on the Atlantic Oceanographic and Meteorological Laboratory web page (www.aoml.noaa.gov/phod/floridacurrent/) and are funded by the DOC-NOAA Climate Program Office-Ocean Observing and Monitoring Division. The mean transport through the Florida Straits averaged during the PEACH experiment is 31.7 Sv (±3.1 Sv) and ranges between 22 and 41 Sv over these 19 months. Variability has peaks at periods of 29 and 14 days, with some peaks at longer (67 day) and shorter (9 and 6.8 day) periods as well (Figure 4).

3. Methods

3.1. Inferring Thermocline Depth From CPIES Acoustic Travel Time

Due to the dependence of sound speed c on temperature and salinity, τ_{950} is a strong function of a CPIES's overlying temperature profile $T(z)$ and to a lesser extent the salinity profile $S(z)$.

$$\tau_{950} = \int_0^{950} \frac{2}{c\rho g} dp \quad (1)$$

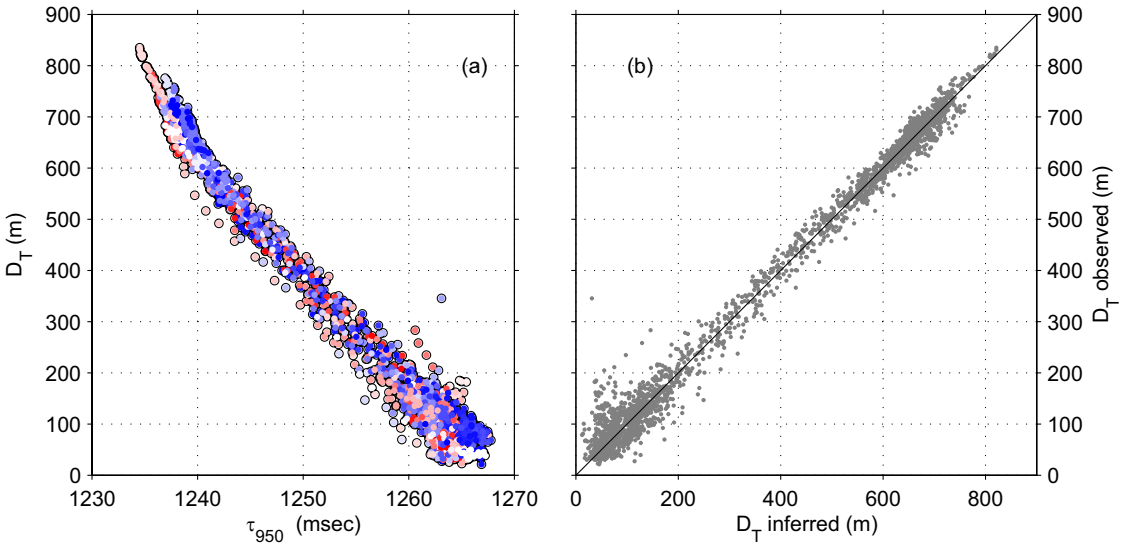

Figure 5. Panel (a): relationship between the depth of the 15°C isotherm (measured) and τ_{950} (calculated), with both determined from Spray glider dives, color-coded by yearday (red is summer, blue is winter, white is spring or fall). Panel (b): comparison for each glider dive of the glider-inferred D_T (using the multi-index lookup table) with the glider-observed D_T (from the dive's hydrographic profile).

Here p is the pressure, which is zero at the sea surface and 950 dbar at the reference level, ρ is seawater density, and g is acceleration due to gravity.

In a strongly sheared current like the Gulf Stream, variability in acoustic travel time is dominated by changes in the thermocline depth D_T. At a given site, D_T can vary for two main reasons. First, for a current that is fixed in space, a local change in the current's vertical shear ($\partial u/\partial z$, $\partial v/\partial z$) is accompanied by a change in the thermocline slope across the current ($\partial D_T/\partial y$, $\partial D_T/\partial x$), with stronger shear associated with a steeper slope, as described by the thermal wind relationship. Second, D_T can change as a current with fixed vertical structure meanders back and forth across a site. In either case, a deeper thermocline is associated with more warm water overlying a CPIES site, and hence shorter τ_{950}. To quantify this expected negative correlation between D_T and τ_{950} for a specific region, hydrographic observations from that region can be used to generate an empirical lookup table (e.g., Watts et al., 1995).

For the PEACH CPIESs, this lookup table is developed using temperature and salinity profiles from 2,672 Spray glider dives that reach to at least 950 dbar to establish the relationship between τ_{950} and the depth of the 15°C isotherm, which serves as a good marker for the thermocline in the Gulf Stream. The location of the 15°C isotherm at 200 dbar has been used widely as a proxy for Gulf Stream position, as this tends to track the location of the maximum surface current (Fuglister & Voorhis, 1965; Sanchez-Franks et al., 2014). The profiles from the glider dives fall within a box centered around Cape Hatteras (34–38°N, 70–78°W) and span 2004 through 2020, with most collected during the PEACH experiment period (Heiderich & Todd, 2020; Todd, 2020a, 2020b; Todd & Owens, 2016). Each dive's temperature and salinity profiles are used both to find D_T for that profile and to calculate τ_{950} from Equation 1, using the glider-measured water properties along with the equation for sound speed in seawater to determine c.

The glider-derived D_T and τ_{950} confirm that a deep thermocline is associated with shorter τ_{950} (Figure 5a), as expected. There is scatter in the relationship, some of which is due to seasonal variability in temperature of the upper ocean (<100 dbar) that manifests in τ_{950} but varies independently of D_T. The magnitude of this seasonal contribution to τ_{950} variability is about 1 ms. Although this is relatively small compared to variability due to thermocline displacements (about 30 ms), a seasonal correction is applied by implementing a multiindex lookup table from which D_T is inferred from a combination of τ_{950} and yearday.

For this multi-index lookup table, all profiles taken within a ±30-day window around a given yearday (1–365) are used to establish that yearday's relationship between D_T and τ_{950} using a cubic spline fit. Since the

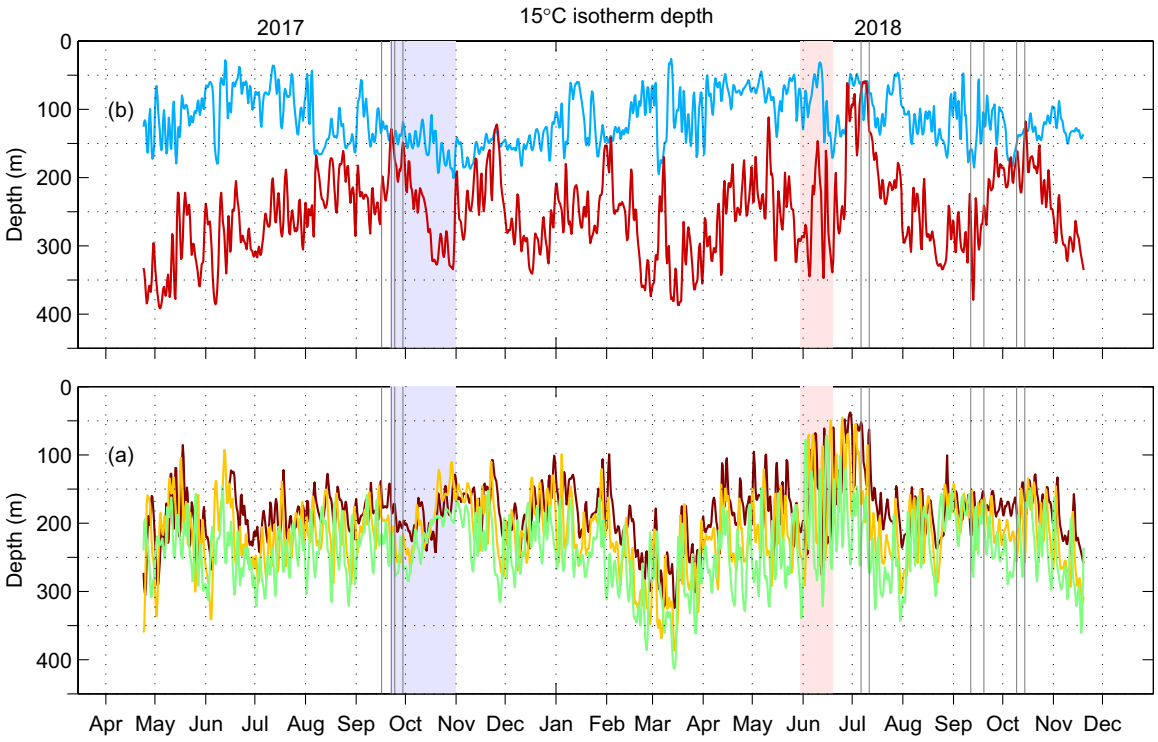

Figure 6. Panel (a): thermocline depth D_T along the Gulf Stream at the sites approaching Cape Hatteras from south to north at P7 (green), P6 (yellow), and P5 (red). Panel (b): thermocline depth D_T across the Gulf Stream just downstream of Cape Hatteras at P1 (blue) and P2 (red). Shading highlights periods of particularly low (blue) and high (pink) variability in the 3–22-day band as in Figure 3. Vertical lines span times when hurricane events were in the PEACH region: Jose, Maria, Chris, Florence and Michael.

gliders provide excellent seasonal coverage, each yearday's lookup table is based on at least 334 hydrographic profiles.

Using the multi-index lookup table, time series of D_T are obtained at each CPIES site from τ_{950} and yearday. This allows characterization of D_T along the cyclonic flank of the Gulf Stream at the three sites approaching The Point east of Cape Hatteras (Figure 6a) and across the cyclonic flank of the Gulf Stream at the two sites just downstream of The Point (Figure 6b).

To obtain estimates of the uncertainties in the 15°C isotherm depths inferred from the CPIES observations using this multi-index lookup table, the glider-observed D_T is compared with the corresponding glider-inferred D_T, where the latter is obtained from each cast's calculated τ_{950}, the yearday of the glider dive, and the lookup table (Figure 5b). The root mean square difference (rms error) between the inferred and observed D_T is 28 m (calculated from 2,349 casts). Much of this overall error is due to those casts that are within the Slope Sea, onshore of the Gulf Stream where the thermocline is often shallower than 250 m depth. For those profiles with D_T less than 250 m, the rms error is 35 m, based on 1,040 casts. For those casts that sample a deeper thermocline, as is generally found within the Gulf Stream and Sargasso Sea, the rms error is smaller: 20 m (based on 1,309 casts). This smaller error estimate (20 m) is suitable for sites P2, and P5–P7, whereas the larger error estimate (35 m) is suitable for P1, which is in the southwestern-most Slope Sea and often shoreward of the Gulf Stream.

3.2. Inferring Meander Amplitude From τ_{950} Assuming a Fixed Gulf Stream Structure

Halkin and Rossby (1985) report that the meandering Gulf Stream at 73°W has "a very well defined dynamical structure which maintains its integrity regardless of its instantaneous position." Due to this Gulf Stream "stiffness," the time-varying D_T at a given site can be used to infer the instantaneous cross-stream distance X to the core of the meandering current as it sweeps over the site (Hall & Bryden, 1985; Johns et al., 1995).

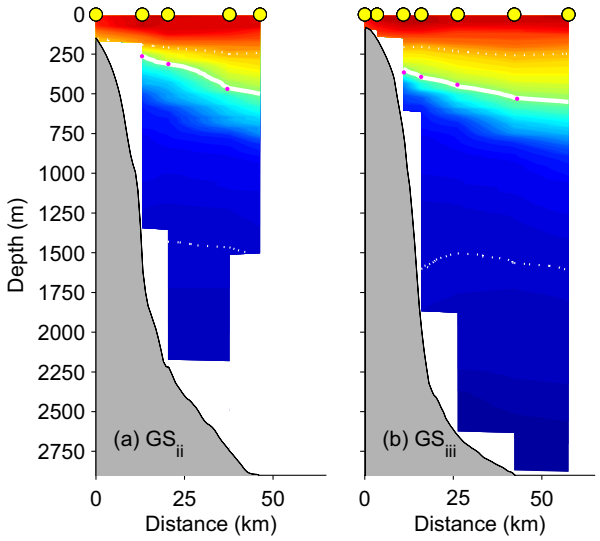

Figure 7. Temperature sections across the Gulf Stream where it approaches The Point (i.e., upstream of the separation location near Cape Hatteras). Cross-stream spacing between casts X is indicated with the yellow circles. The 15°C isotherm is highlighted with the solid white curves. For comparison, the 4°C and 20°C isotherms (dotted white) are also shown. Those thermocline depths used to obtain the estimate of $\partial D_T/\partial$ between pairs of casts are highlighted in magenta.

Taking advantage of this well-defined dynamical structure, and further assuming that the thermocline slope varies little as the Gulf Stream meanders over the steep topography, rough estimates of the amplitude of wave-like Gulf Stream meanders can be obtained for sites P5-P7 by converting the CPIES-inferred D_T records into a measure of offshore/onshore changes in Gulf Stream position. For this, the structure of the Gulf Stream is characterized using two temperature sections taken across the current where it approaches Cape Hatteras just upstream of The Point (Figure 6). These hydrographic sections (GS$_{ii}$, GS$_{iii}$) are used to estimate a time-invariant thermocline slope across the Gulf Stream $\partial D_T/\partial X$ on its approach to the (time-varying) separation location. These sections are from shipboard surveys, taken with a Sea-Bird Electronics SBE 911plus/917plus CTD from the *R/V Neil Armstrong* during the PEACH deployment cruise AR15 in April 2017 (Andres et al., 2018). Each section took about 10 h to complete, crosses perpendicular to the isobaths where the continental slope is steepest, and lies roughly perpendicular to the Gulf Stream flow within 130 km of The Point. Although additional historical hydrographic sections across the Gulf Stream are available up- and downstream of this region approaching The Point, these are not used here to estimate $\partial D_T/\partial X$ because the mean Gulf Stream structure (transport and water classes carried in the current) varies strongly in the downstream direction (Heiderich & Todd, 2020).

The estimate for $\partial D_T/\partial X$ obtained from sections GS$_{ii}$ and GS$_{iii}$ is 6.4 m/km ±1.8 m/km (with the error estimated from the standard deviation of the slope between neighboring shipboard casts). This $\partial D_T/\partial X$ is used as a conversion factor to infer the time-varying amplitude A of wave-like Gulf Stream meanders from CPIES-inferred D_T at sites P5–P7 (see Section 5.1) and to examine how Gulf Stream meanders are modulated as they approach The Point. For these wave-like meanders, it is assumed that D_T variability captured by the CPIESs (in the 2–15-day band) is primarily due to changes in Gulf Stream lateral position rather than changes in the current's vertical structure or transport.

4. Results

Using the datasets and methods described above, mean and time-varying Gulf Stream path is characterized spanning The Point east of Cape Hatteras. Gulf Stream variability up- and downstream of the time-varying separation location, where the Gulf Stream veers away from the continental margin, is examined across temporal scales to investigate wave-like meanders as well as lower-frequency variability associated with Gulf Stream transport anomalies and path shifts.

4.1. Gulf Stream Position: Means and Distributions Spanning The Point

The Gulf Stream's separation location generally falls within the gap between the satellite tracks spanning Cape Hatteras. Comparison of the bathymetry around Cape Hatteras to time averages of the Gulf Stream position inferred from |δSSH/δx|, confirms that the Gulf Stream crosses isobaths here (blue and green circles in Figure 2). These Gulf Stream positions inferred from the along-track satellite data are consistent with the mean Gulf Stream path inferred from a constant 25.1-cm SSH contour in the time-averaged mapped SSH (red curve in Figure 2).

The slope of the bathymetry and the proximity of the shelf break likely both play an important role in controlling the distribution of Gulf Stream positions up- and downstream of The Point at the respective satellite tracks. The mean position of the Gulf Stream at track-152 (i.e., approaching the separation location) sits over the 2670-m isobath, where the bottom slope is about 50 m km^{-1} (5% grade) The distribution of Gulf

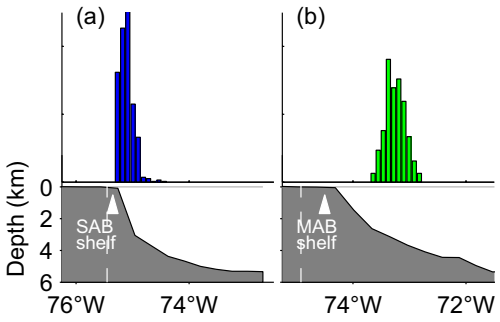

Figure 8. Histogram of Gulf Stream core positions from 1993 through mid-2019 at (a) track-152 by the South Atlantic Bight (SAB) shelf and (b) track-228 by the Middle Atlantic Bight (MAB) shelf. In each plot, the dashed line indicates the location of the coast.

Stream core locations inferred from |δSSH/δx| is asymmetric with only small onshore displacements and a few very large offshore excursions in which the core is displaced up to 150 km (to the 4300-m isobath) from its mean position (Figure 8a). The magnitude of the onshore excursions is limited to about 45 km, which brings the core of the Stream close to the 100-m isobath on the outer edge of the SAB shelf. Downstream of this, where the Gulf Stream reaches track-228, the mean core position is found over the 3,350 m isobath, which is about 115 km offshore of the MAB shelf break and the bottom slope is about 10 m km^{-1} (1% grade). The distribution of core positions over the gentle slope here is symmetric and wider, with ±90-km shifts on- and off-shore of the mean (Figure 8b). The core is largely contained between the 2,500 and 4,000-m isobaths.

4.2. Gulf Stream Variability Inferred From the CPIESs at Periods From Days to Months

With this regional context about the Gulf Stream path envelope inferred from the along-track altimetry, the CPIESs' 2-day low-pass filtered τ (Figure 3) and D_T derived from this (Figure 6) are used to characterize Gulf Stream variability at periods from days to months. Using spectral analysis of τ and its derived quantities, the character of Gulf Stream variability up- and downstream of the separation location by Cape Hatteras is examined to identify wave-like meanders and variability associated with low frequency Gulf Stream shifts and transport changes. Calculations of (lagged) correlations between D_T (or equivalently, τ_{950}), give evidence of signal propagation. Coherence and phase estimates are used to calculate the wavelength λ and phase speeds c_p of the signals in various frequencies bands.

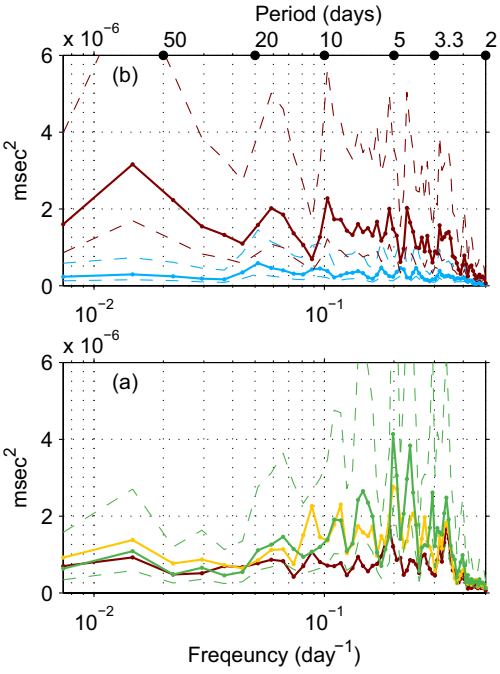

Figure 9. Variance preserving spectra of τ at the CPIES sites (a): approaching Cape Hatteras from south to north at P7 (green), P6 (yellow), and P5 (red), and (b): just downstream of Cape Hatteras at P1 (blue) and P2 (red) calculated with a 136-day window and 50% overlap. Dashed lines indicate the respective 95% confidence limits (only included for P7 in (a), for clarity).

4.2.1. Spatial Distribution of Gulf Stream Variability Spanning The Point

On the Gulf Stream's approach to The Point east of Cape Hatteras, there is little energy in the mesoscale band (30–100 days). Rather, much of the τ variance at sites P7, P6, and P5 occurs at periods shorter than 25 days (Figure 9a) and this variance decays markedly at all frequencies as the Gulf Stream approaches P5. This is consistent with previous studies that have reported a decrease in the Gulf Stream wave-like meander amplitudes between the Charleston Bump and Cape Hatteras (e.g., Lee et al., 1991; Miller, 1994) and suggests that this damping continues right along the Gulf Stream's final 140-km approach to The Point.

As the Gulf Stream continues from P5 past The Point to P2, the frequency fingerprint changes dramatically from a red spectrum to a blue one even though P5 and P2 are separated by only 60 km. Variance in τ is higher at P2 than at P5 in all frequency bands (compare the red curves in Figures 9a and 9b), but the increase in mesoscale variability is particularly pronounced, with a broad peak at P2 centered around 65 days. Variance in τ at P1 is relatively low at all frequencies (Figure 9b) and this site usually falls onshore of the energetic, meandering Gulf Stream, outside of the Gulf Stream cyclonic flank in a region where the thermocline is relatively flat.

Guided by this spatial pattern of variability around Cape Hatteras, established from the variance preserving spectra of the minimally processed CPIES τ records, the derived components (D_T and A) are examined in more detail to study signal propagation approaching The Point and spanning the separation location.

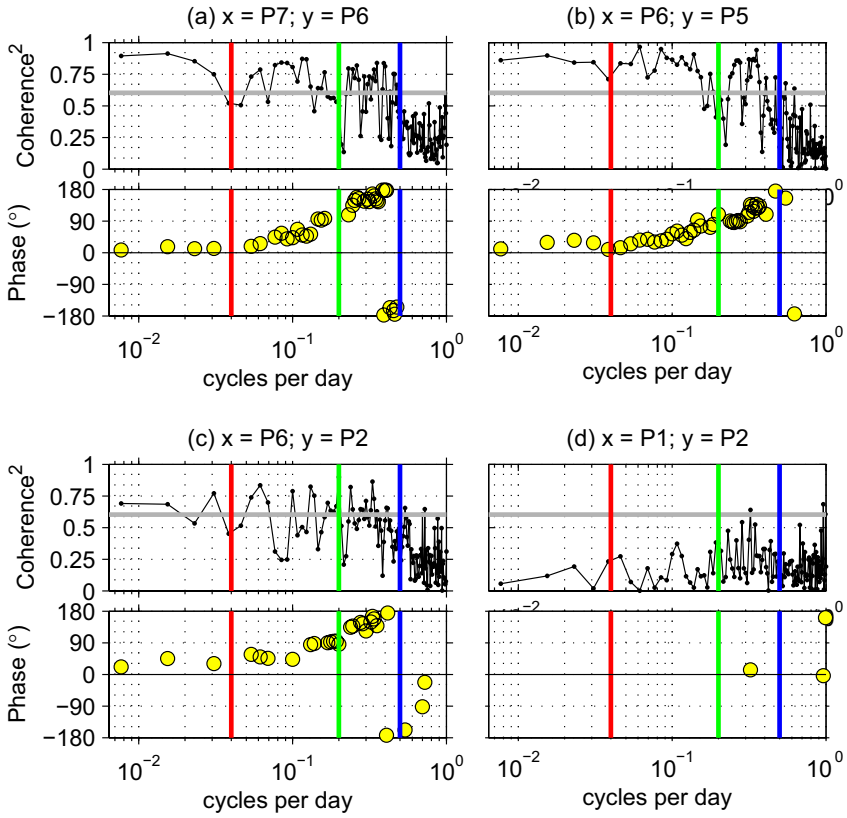

Figure 10. Magnitude squared-coherence (top panels) and phase (bottom panels) for various pairs of CPIESs. These are calculated for concurrent records of D_T with 522.5-day duration (linearly detrended), using 130-day Hamming windows with 50% overlap. Phase is only shown for frequencies whose squared-coherence is significant at or above the 99% confidence limit assuming six equivalent degrees of freedom (Emery & Thomson, 2004). The equivalent degrees of freedom are based on the record length and window length (Thompson, 1979), adjusted slightly to account for the window overlap and window shape. Vertical lines indicate 2-day (blue), 5-day (green), and 25-day (red) period. Positive phase means that x leads y (note that close to ±180° the signal can wrap).

4.2.2. Which Signals Move Downstream Past The Point?

The D_T records (i.e., thermocline depths) are strongly lag-correlated with one another at all CPIES sites except P1. Though the separation between P1 and P2 is only 30 km, these D_T records are uncorrelated since they straddle the sharp front of the Gulf Stream North Wall and hence generally "see" environments with very different energetics, namely the Slope Sea at P1 and the Gulf Stream cyclonic flank at P2. For the remaining sites, which generally fall within the Gulf Stream cyclonic flank, strong correlation is observed even between those sites that span The Point. For example, for P5 and P2, correlation r peaks at 1.5-day lag, reaching $r = 0.72$. Lags suggest the signals move downstream from P7, past P6 and P5, and toward P2 at about 40 km d^{-1} (0.5 m s^{-1}), which is slower than the Gulf Stream core speed (2 m s^{-1}), but faster than the propagation of large amplitude Gulf Stream meanders east of 73°W where the crests and troughs can stall completely or move eastward at speeds reaching only around 0.1 m s^{-1} (Cornillon, 1986).

These lagged correlations include the combined influence from all frequencies. To separate the various processes that contribute to D_T variability and to evaluate whether there is downstream evolution of the signals, magnitude-squared coherences and phases are examined. Calculations of coherences and phases of D_T between pairs of instruments show downstream propagation across a broad range of frequencies on the approach to The Point, with periods of significant peaks spanning 2–130 days (Figures 10a and 10b). However, only the high-frequency signals (i.e., those with periods less than 25 days) are significantly coherent at the 99% confidence level across the separation location, spanning the 112-km distance between P6 and P2 (Figure 9c) or the 175-km distance from P7 to P2 (figure not shown). In contrast, the signals with periods

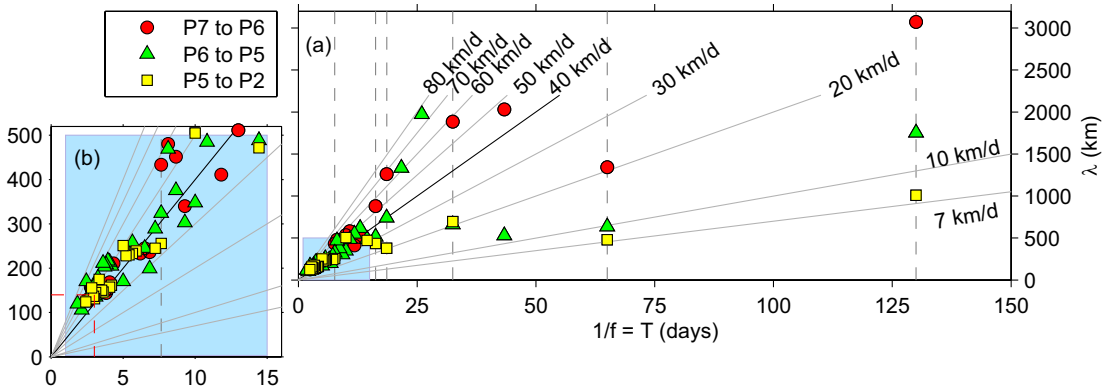

Figure 11. Panel (a): dispersion diagram showing the relationships between T (=1/f) and λ calculated between neighboring pairs of CPIESs according to Equation 3. Solid lines indicate lines of constant c_p with 40 km d^{-1} emphasized (heavy line). Blue shading highlights wave-like meanders with $\lambda < 500$ km and T < 15 days. Vertical dashed lines indicate those periods at which the signals appear to slow and shorten as they move downstream past the separation location from P7 toward P2 (7.6, 16, 19, 32, 65, and 130-day period). Panel (b): closeup of the wave-like Gulf Stream meanders with symbols as in (a). T = 40-day period is highlighted with the dashed red lines.

longer than 25 days do not tend to propagate downstream across the separation location from P7 (or P6) to P2. There is, however, some evidence of coherence–even at these periods longer than 25 days across the shorter distance (60 km), separating P5 and P2. D_T at P1 is not coherent with that at any of the other sites (Figure 10d), consistent with the lagged correlation calculations.

Wavelengths of those signals with a statistically significant coherence peak are estimated from the phases between neighboring CPIESs according to:

$$\lambda = \frac{d360°}{\phi} \tag{2}$$

where λ is the wavelength, ϕ is the phase lag for the given coherence peak, and d is the distance between instruments (Watts & Johns, 1982). From this, the associated phase speed c_p is calculated according to:

$$c_p = \lambda f \tag{3}$$

where f is the frequency of the peak (f = 1/T where T is the period).

For wave-like Gulf Stream meanders, categorized here as those signals with $T < 15$ days and $\lambda < 500$ km (blue shading in Figure 11), the longer wavelength signals tend to have longer period (lower frequency). These wave-like meanders propagate in the direction of Gulf Stream flow, with c_p of about 30–70 km d^{-1}, in agreement with the phase speed estimated above from the lagged correlations (40 km d^{-1}). These wave properties are consistent with previously reported values of Savidge (2004) who observed 3–8-day wave-like Gulf Stream meanders approaching The Point having 180–380-km wavelength and 40–55 km d^{-1} downstream phase speed. These findings are also broadly consistent with modeled and observed phase speeds of propagating meanders between the Charleston Bump and Cape Hatteras (Gula et al., 2016 and references therein). Except at 7.6-day period (discussed further in Section 4.2.3), it is difficult to discern consistent decrease in c_p or shortening of λ of these wave-like Gulf Stream meanders as they propagate through the PEACH CPIES Array approaching The Point and then passing the separation location. Such a slowdown and shortening of waves approaching Cape Hatteras (as noted in Savidge, 2004), likely occurs slightly upstream, before the waves reach the PEACH CPIESs at the Gulf Stream's final approach toward The Point (e.g., see Figure 1b and discussion in Section 4.2.3).

Signals with longer period ($T > 50$ days) tend to move downstream between neighboring CPIES sites more slowly than the wave-like Gulf Stream meanders do. For these long-T, large-λ signals, downstream phase speed of D_T is less than 20 km d^{-1} (Figure 11). In addition to this tendency for long-period signals to move slowly compared to the propagation of wave-like meanders, there is a clear spatial dependence of c_p for the long-period signals. For a given T, signal propagation is slower downstream of the separation location (i.e.,

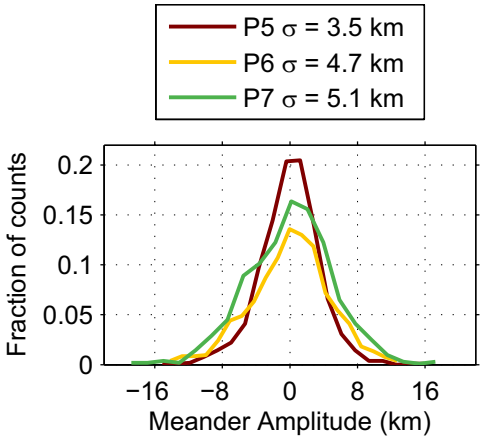

Figure 12. Probability density function of A at the three CPIES sites approaching The Point.

where signals move from P5 to P2) than it is on the approach to the separation location (i.e., where signals move from P7 to P6 or from P6 to P5).

4.2.3. Changes in Wavelength and Phase Speed Spanning The Point

Taking a broader view, it is evident that wavelength changes as signals approach and then pass The Point. An SST snapshot from June 4, 2018 (Figure 1b) shows an undulating front between 28°C water (red) and 26°C water (orange) that captures two complete cycles with wavelength about 70% longer approaching The Point ($\lambda_1 \sim 200$ km) than just downstream of The Point ($\lambda_2 \sim 140$ km). Though it cannot be determined from this single snapshot (and these wave crests are not clear in the neighboring days' snapshots, due to cloud-cover), the relationship in Figure 11b suggests that 140-km waves have about 3-day period.

Although the PEACH CPIES Array is not able to consistently resolve this for all of the wave-like meanders ($T < 15$ days, $\lambda < 500$ km), this decrease in λ spanning The Point inferred from SST is consistent with Savidge (2004) and is confirmed here by some of the coherence and phase calculations based on neighboring CPIES records. These indicate that some signals slow (and shorten) as they pass The Point (Table 2). For signals approaching Cape Hatteras with $\lambda > 500$ km, waves are consistently slower and their λ shorter downstream of The Point than they are upstream of The Point. For example, waves with 65-day period, travel at $c_p = 20$ km/day between P7 and P6 and have $\lambda = 1{,}340$ km. Between P6 and P5, these waves are slower ($c_p = 10$ km day^{-1}) and shorter ($\lambda = 640$ km). Finally, between P5 and P2 they are even slower and shorter with $c_p = 7$ km d^{-1} and $\lambda = 480$ km (Figure 11, compare red circle, green triangle and yellow square at $T = 65$ days).

Likewise, at $T = 130$ days, c_p decreases from 24 km d^{-1}, to 13 km d^{-1}, to 8 km d^{-1} as λ decreases from 3,072 to 1,750 km, and finally to 1,010 km (Table 2 and Figure 11). At such long "wavelengths," however, the signals span a distance greater than the 1,100 km separating the Florida Straits from Cape Hatteras, so it is perhaps better to envision these lateral displacements as whole-sale shifts of the Stream, rather than wave-like meanders propagating along the core of the Gulf Stream.

There is a less consistent downstream pattern in the wave-like meanders observed here (i.e., those waves with $\lambda < 500$ km). In some cases, they also appear to slow and shorten as they approach and pass The Point. For example, the 7.6-day period waves slow (from 57 to 33 km d^{-1}) and shorten (from 433 to 256 km) by about 40% approaching and then passing The Point (Table 2). At other frequencies, however, this pattern is not clear in these data. Since an actual meander in the Gulf Stream path is likely not truly sinusoidal, a given meander pattern will manifest in the spectrum as a combination of several sine components of differing wavelength. As the meander pattern progresses northeastward, the various components may travel at different speeds, so as to combine and give the spatially varying physical pattern that is observed in an SST image.

5. Discussion

The 19-month PEACH CPIES acoustic travel time records capture variability in the depth of the thermocline across a wide range of temporal scales. In principle, D_T variability at a given CPIES site can conflate the influence of Gulf Stream position changes with the concurrent influence of Gulf Stream transport anomalies and the associated changes to the thermocline tilt. To distinguish these separate contributions to overall D_T variability, different frequency bands are considered individually and auxiliary data sets are used to aid in the interpretation of the D_T records within these different frequency bands.

5.1. Gulf Stream Wave-Like Meanders

The amplitudes of wave-like Gulf Stream meanders at P7–P5 can be estimated using the canonical Gulf Stream temperature sections (Figure 7) and a conceptual model in which this fixed structure meanders back

Table 2
Evidence of D_T Signal Modulation Approaching and Passing The Point

T (days)		P7–P6	P6–P5	P5–P2
130	c_p (km day^{-1})	24	13	8
	λ (km)	3072	1753	1009
65	c_p (km day^{-1})	21	10	7
	λ (km)	1343	637	479
32	c_p (km day^{-1})	59	22	21
	λ (km)	1884	695	661
19	c_p (km day^{-1})	68	40	20
	λ (km)	1261	741	379
16	c_p (km day^{-1})	54	32	27
	λ (km)	880	516	435
7.6	c_p km day^{-1})	57	45	33
	λ (km)	433	342	256

and forth across a CPIES site. This simple model assumes that acoustic travel time variability in the 2–15-day band is primarily related to changes in Gulf Stream position rather than to changes in Gulf Stream transport or vertical structure. This simplification is supported by upstream measurements in the Florida Straits, where 3–30-day period Gulf Stream meanders observed with HF radar have 8-km standard deviation and a prominent spectral peak at 9-day period, but only a small corresponding 9-day spectral peak in Gulf Stream transport (Archer et al., 2017). The latter was inferred from the cable measurements across Florida Straits (Meinen et al., 2010) and is confirmed here specifically for the PEACH time period by calculating the variance preserving spectrum of daily Florida Current transport between April 2017 and November 2018 (Figure 4b). This suggests that at least some of the wave-like meanders in the Straits represent position variably that is largely independent of Gulf Stream transport variability, and it is assumed here that the same is true near Cape Hatteras.

Near Cape Hatteras, wave-like Gulf Stream meander amplitudes A are inferred from the 2–15-day band-passed D_T records divided by the thermocline slope, 6.4 m km^{-1}. The time series of A at each CPIES site, suggests that the meanders, quantified by the standard deviation σ of A (Table 3), decrease by 30% from P7 ($\sigma = \pm 5.1$ km) to P5 ($\sigma = \pm 3.5$ km). This lower σ is evident also in the narrower histogram of A at P5 than at P6 or P7 (Figure 12).

In addition to the spatial decay of meander amplitude on the approach to The Point, the intensity of Gulf Stream meandering near Cape Hatteras varied temporally during the PEACH experiment period. Meander amplitudes at sites P7–P5 and P2 are particularly small during October 2017 and large during late-May/June 2018 (see the shaded regions in Figure 3). On May 31, 2018 as a meander crest passes by P7, the Gulf Stream shifts onshore by 17.4 km. By June 2, the meander trough arrives at P7 and shifts the Gulf Stream offshore by 19.7 km, resulting in a 37.2-km peak-to-peak translation of the GS core by this meander passage (Figure 13). To examine possible causes of the variability in meander intensity at Cape Hatteras, both local and remote conditions are considered.

Variability in the intensity of the Gulf Stream meandering does not seem to be forced by the local winds. Wind stress near Cape Hatteras is characterized by a "cool season" with strong winds associated primarily with passing extra-tropical cyclones, and which typically runs from mid-September through the end of April. Conditions transition rather abruptly to a "warm season" from May to mid-September when winds are typically weak and from the southwest, and are only occasionally punctuated by strong tropical cyclone events (Bane et al., in preparation, 2021). Counter-intuitively, the largest meander amplitudes recorded by the CPIESs occurred during the 2018 warm season when the local winds were weak, and the smallest meander amplitudes coincided with the windy 2017–18 cool season (Figure 13).

Table 3
Characteristics of Gulf Stream Wave-Like Meanders Approaching The Point East of Cape Hatteras

	2–15-day band		2–8-day band	
	A (km)		A (km)	
	σ	Max.	σ	Max.
P5	±3.5	±16	±2.8	±15
P6	±4.7	±14	±3.6	±13
P7	±5.1	±19	±4.0	±16

Note. For consistency, the estimates at each site are made over the period June 15, 2017 through November 19, 2018 to avoid the beginning of the record at P5 when there was a short data gap.

Mapped SSH suggests that the variability of meander intensity in the Gulf Stream near Cape Hatteras is not correlated to the local SSH around Cape Hatteras nor to the SSH along the SAB, but that it may be related to conditions about 1,400 km upstream in the Gulf of Mexico. The path of the Loop Current in the eastern Gulf of Mexico varies between expanded and contracted states related to the growth and shedding of Loop Current Eddies, which detach and then typically move westward through the Gulf (compare the dark red and magenta curves in Figure 14). The frequency of this eddy-shedding cycle is irregular but occurs, on average, at about 8–9-month intervals (Leben, 2005).

The time-varying meander intensity near Cape Hatteras is quantified here with the standard deviation of A (σ) at P7 within a moving 22-day

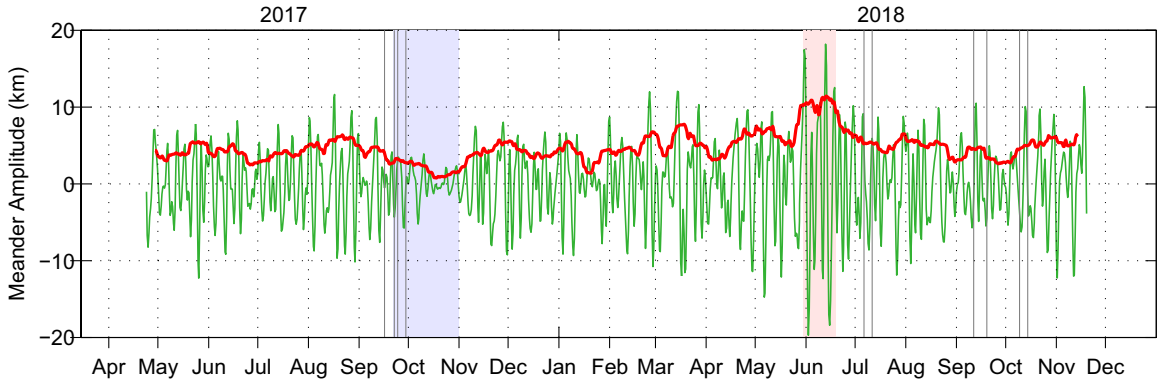

Figure 13. Time-varying intensity (red curve) of wave-like Gulf Stream meander amplitude A at P7 (green). Blue and pink shading show times of particularly low and high intensity, respectively. Vertical lines span times when hurricane events were in the PEACH region: Jose, Maria, Chris, Florence, and Michael.

window (Figure 13, with similar time series for P6 and P5 not shown). A correlation map of this meander intensity with SSH suggests that the most intense wave-like meanders off Cape Hatteras may be related to a Loop Current transition in the eastern Gulf of Mexico. When meander activity east of Cape Hatteras is high (i.e., when there is large standard deviation in the 2–15-day band-pass filtered Gulf Stream position inferred from the CPIESs), SSH is high in the eastern Gulf of Mexico where the Loop Current extends northward into the Gulf of Mexico prior to an eddy-shedding event (Figure 14c). Before they slow on their approach to Cape Hatteras (Savidge, 2004), wave-like Gulf Stream meanders are observed to have phase speeds around 80 km d^{-1} through Florida Straits and along the SAB (Archer et al., 2017). At this speed, and if they are non-dispersive, meanders would be expected to take about 18 days to propagate from the eastern Gulf of Mexico to Cape Hatteras.

This delay suggests that the wave-like meanders may be excited during the Loop Current's northward expansion prior to reaching the fully expanded state that precedes the eventual eddy shedding. This is consistent with lagged-correlation maps: at 40-day lead, SSH in the eastern Gulf of Mexico shows no correlation with meander intensity at Cape Hatteras and there is no signature yet of Loop Current expansion (Figure 14a). By 15-day lead, however, the SSH correlation pattern emerges (Figure 14b) and suggests that it is SSH variability near the Southwest Florida shelf break that may excite the intense wave-like meanders that eventually arrive at Cape Hatteras. Meanwhile as these then propagate toward Cape Hatteras, Loop Current expansion continues (Figures 14c and 14d) and eventually an eddy is shed about 40 days after the peak in meander amplitude at Cape Hatteras (Figure 14e).

5.2. Gulf Stream Thermocline Depth and Florida Current Transport

In contrast to the D_T variability associated with changes in Gulf Stream position due to the wave-like meanders discussed above, some low frequency signals captured by the CPIES-inferred D_T records are instead primarily driven by changes in Gulf Stream transport off Cape Hatteras. Forty-day low-pass filtered D_T decreases by almost 200 m at P7–P5 over the course of 4 months from March through June 2018 (Figure 15b). Coincident with this shoaling thermocline within the cyclonic flank of the Gulf Stream along the SAB where the Gulf Stream approaches The Point, 40-day low-pass filtered transport through the Florida Straits observed with the submarine cable measurements increases by about 8 Sv (black curve). An analogous relationship is evident near the beginning of the records from May through the end of June 2017, when D_T increases by 35 m as Florida Current transport decreases from 34 to 31 Sv.

These correspondences between Florida Current transport and D_T at sites just upstream of The Point suggest that the four-month long decrease of D_T reflects primarily changes to the thermocline slope across the (spatially fixed) Gulf Stream instead of a slow offshore-shift of the Gulf Stream path during this time period. In this scenario, since P7–P5 are each located on the onshore side of the thermocline's pivot point, as D_T at these sites decreases (becomes shallower) the thermocline at the offshore edge of the Gulf Stream would

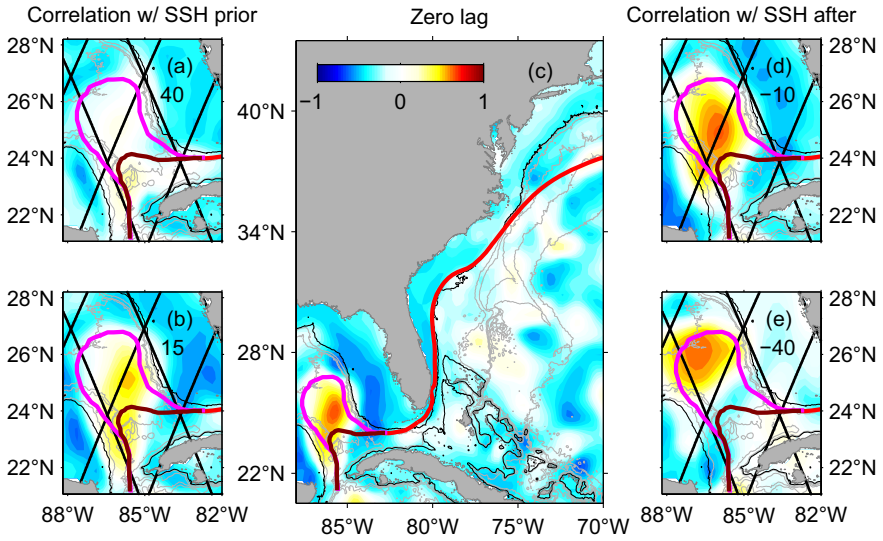

Figure 14. Lagged-correlation maps generated by comparing meander intensity at Cape Hatteras (as quantified by the red curve in Figure 13) with sea surface height (SSH) in the western North Atlantic and Gulf of Mexico. Each panel indicates the lag (in days) between SSH and the intensity; positive (negative) lags show the correlation with the SSH pattern prior to (after) the measure of meander intensity at Cape Hatteras. Correlations are calculated after linearly detrending each time series. Also shown are the mean Gulf Stream path from the 25.1-cm SSH contour (red), and schematics of the Loop Current in an extended (magenta) and retracted (dark red) state.

be expected to either remain steady or deepen during a transport increase. The correlation between Florida Current transport and D_T at P7 (with both records 40-day low pass filtered) is −0.43, so almost 20% of the variance in D_T at P7 at periods longer than 40 days is tied to transport changes in the Florida Straits (Figure 15c, green), with similar relationships found at P6 and P5 (figure not shown). A regression of Florida Current transport onto thermocline depth suggests that coincident with every 1 Sv increase of Gulf Stream transport through the Florida Straits, D_T on the cyclonic flank of the Gulf Stream approaching The Point shoals by 5 m. (As an aside, there is also substantial low-frequency D_T variance here that *is* related to position changes: more than 25% of the D_T variance at P7 is tied to concomitant 40-day low-pass filtered position changes observed at the nearby satellite track-152, but those position changes, in turn, are not significantly correlated with Florida Current transport, Figure 15c, dashed gray.)

A strongly tilted thermocline is the hallmark of a strongly vertically sheared, high-transport state in the Gulf Stream and is expected to co-occur with a stronger SSH gradient across the Stream that is essentially a mirror image of the thermocline (i.e., enhanced SSH-low on the shoreward side and enhanced SSH-high on the seaward side of the current). To investigate if the 40-day low pass filtered D_T signals that are anti-correlated with Florida Current transport are also related to Gulf Stream transport anomalies near Cape Hatteras (rather than Gulf Stream position changes), the pattern of correlation between SSH and Florida Current transport during the 19-month PEACH experiment is considered. The zero-lag correlation map (Figure 15a) shows that high transport through the Strait (40-day low pass-filtered) is accompanied by decreased SSH along the shoreward side of the Gulf Stream stretching from Florida to Cape Hatteras and increased SSH on the seaward side. This pattern of stronger SSH gradient across the Stream indicates that during times of low D_T (shallow thermocline) approaching The Point, Gulf Stream transport is high not only in the Florida Straits, but along the entire SAB.

This dipole correlation pattern in SSH across the Gulf Stream does not continue beyond Cape Hatteras (Figure 15a). Consistent with this, there is also no significant correlation at zero-lag between Florida Current transport and D_T at P2, which is the CPIES site just downstream of the separation location (Figure 15c, magenta). Apparently, low-frequency Gulf Stream transport anomalies in the Florida Straits and along the SAB are decoupled from those in the separated Gulf Stream. This finding that Gulf Stream flow is not continuous like that in a pipe agrees with previous research in which interannual Florida Current transport variability

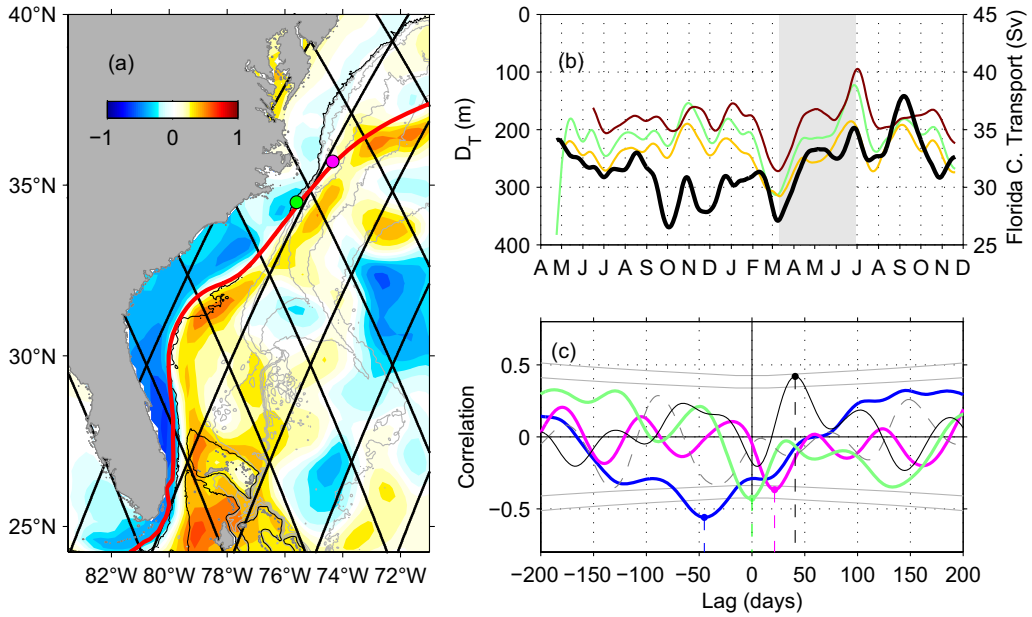

Figure 15. (a) Correlation during the 19-month PEACH experiment period between sea surface height and 40-day low-pass filtered Florida Current transport at zero-lag (here trends have not been removed from either record, but results are similar, regardless). Locations of P2 (magenta) and P7 (green) are indicated. (b) Time series of the 40-day low-pass filtered D_T at P7 (green), P6 (yellow), and P5 (red), and the 40-day low-pass filtered Florida Current transport (heavy black). Shading highlights 4-month period from March through June 2018. (c) Lagged correlations of Florida Current transport with 40-day low-pass filtered D_T at site P7 (green), P2 (magenta), and P1 (blue), with the maximum (negative) correlation highlighted for each. Also shown are lagged correlations between the transport and the offshore distance to the Gulf Stream velocity core at track-152 (gray dashed curve) and at track-228 (solid black curve), with positive correlation indicative of an offshore-shifted Gulf Stream associated with a higher Florida Current transport. Positive lags indicate that Florida Current transport leads; negative lags indicate that Florida Current transport lags. The solid gray curves show measures of correlation significance at the 80% and 90% levels, respectively, taking into account the 40-day low pass filter to estimate the degrees of freedom as a function of the lagged record lengths (i.e., at zero-lag, there are 14 degrees of freedom for the 575-day records, and as lag increases the degrees of freedom decrease).

is not correlated with that near 73°W, with the latter observed with repeat measurements from a shipboard acoustic Doppler current profiler (ADCP) on the CMV Oleander (Sanchez-Franks et al., 2014).

Though a coherent signal associated with Gulf Stream transport anomalies does not seem to extend beyond the separation location, there is evidence that the Gulf Stream downstream of the separation location does "feel" the upstream transport anomalies and eventually responds with a position change that propagates slowly downstream (northeastward) from the separation location. As already noted, Florida Current transport and D_T at P2 are not correlated at zero lag, but they are marginally anti-correlated at 21-day lag ($r = -0.37$, which is significant at the 80% level). Furthermore, Gulf Stream position at track-228 is strongly correlated with Florida Current transport at 41-day lag ($r = 0.42$, significant at the 90% confidence level). The sense of the correlation is such that an offshore shift follows a Florida Current transport maximum by about 41 days. The distance between P2 and track-228 is 125 km, and suggests that this signal propagates downstream at 6 km d^{-1}. This slow signal propagation is similar to the phase speeds inferred from the coherence and phase calculations for signals with long period moving from P5 to P2 (Figure 11, see the yellow triangles at 65- and 130-day period) and is also similar to the speeds of large-amplitude Gulf Stream meanders reported further downstream by Cornillon (1986).

Taken together, the records suggest that 21 days after a positive regional-scale Gulf Stream transport anomaly that stretches along the SAB from Florida Straits to Cape Hatteras, D_T at P2 decreases, not because of a local transport anomaly, but rather because the separated Gulf Stream shifts offshore. Then this Gulf Stream "undulation" moves downstream at about 6 km day, far slower than either the advection in the Gulf Stream velocity core or the propagation of wave-like Gulf Stream meanders (described in Section 4.2.2), but

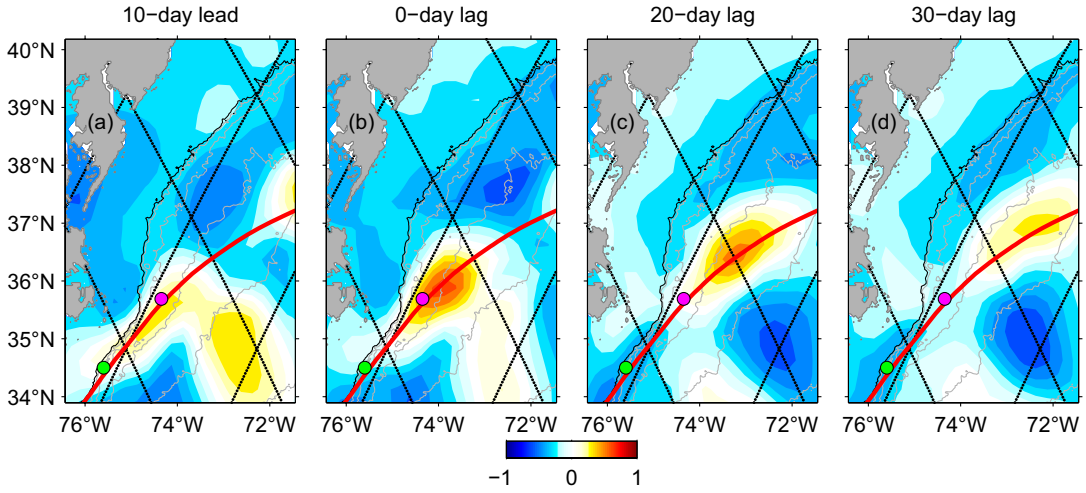

Figure 16. Lagged correlations between sea surface height (SSH) and 40-day low pass filtered D_T at P2: (a) SSH leads D_T at P2 by 10 days (which corresponds to the SSH pattern 10 days after a minimum in Florida Current transport), (b) at zero lag (i.e., 20 days after a minimum in Florida Current transport), (c) with SSH lagging P2 by 20 days (i.e., 40 days after a minimum in Florida Current transport), and (d) with SSH lagging P2 by 30 days (i.e., 50 days after a minimum in Florida Current transport).

at speeds typical of large-amplitude Gulf Stream meanders. Eventually, 41 days after the Florida Current transport anomaly, the undulation is detected in the along-track observations at track-228.

This interpretation, based on D_T, along-track satellite data, and the Florida Current cable measurements, is consistent with the pattern in maps of lagged correlations that compare D_T at P2 with SSH. 10 days prior to a maximum in 40-day low pass filtered D_T at P2, SSH is high along both sides of the mean Gulf Stream path between P5 and P2 (Figure 16a). This pattern is consistent with an onshore-shifted Gulf Stream in the region just upstream of P2. At zero-lag (Figure 16b), the SSH pattern suggests that this slight undulation in Gulf Stream position has moved along the Gulf Stream mean path to P2, such that an onshore Gulf Stream shift is associated with a larger D_T (deeper thermocline) as apparent at P2. The sense of the lagged correlations in Figure 15c, suggests that this zero-lag pattern follows a minimum in Florida Current transport by 20 days. At progressively longer lags (Figures 16c and 16d), this undulation continues to move downstream slowly (and dissipate somewhat), consistent with the speeds inferred above.

6. Conclusions

Consistent with previous research, the PEACH CPIES observations show that the amplitudes of the wave-like Gulf Stream meanders in the 2–15-day band are usually (but not always, recall Figure 13) smaller near Cape Hatteras than observed upstream near the Charleston Bump, where they can reach 40-km amplitude (Bane & Brooks, 1979; Miller, 1994). Furthermore, wave-like Gulf Stream meanders continue to decay on their final approach to the separation location near Cape Hatteras with amplitudes decreasing by about 30% as they propagate along the 140-km section of steep slope connecting P7–P5. Superimposed on this local spatial evolution is temporal variability in the intensity of wave-like meanders, which varies substantially over the PEACH experiment and may be related to shedding of Loop Current Eddies in the Gulf of Mexico. The CPIES records, which span 19 months, are short relative to the average eddy-shedding cycle (8–9 months). A longer study, perhaps capitalizing on HF radars to characterize wave-like Gulf Stream meander-intensity near Cape Hatteras for long duration, would help establish whether the relationship between SSH and meander intensity suggested by the PEACH CPIESs is robust through several Loop Current expansion/eddy-shedding events. Furthermore, there are likely multiple processes which can cause intense wave-like meander activity along the SAB and at Cape Hatteras, such as a cold-core ring interacting with the seaward side of the Stream. Thus, it would be informative to cross-compare long-duration HF radar-based measures of Gulf Stream meander amplitude at multiple sites along the SAB (e.g., near Cape Hatteras and in the Florida Straits) to examine subannual to interannual variability in meander intensity. Substantial

variability in the intensity of wave-like Gulf Stream meanders along the SAB could be indicative of important sub-annual to interannual variability in the nutrient pump (Glenn & Ebbesmeyer, 1994) and strength of shelf-ocean exchange along the entire SAB.

Comparing 40-day low-pass filtered in situ records from the PEACH experiment period (comprising Florida Current transport, satellite along-track Gulf Stream positions, and D_T records) with mapped SSH using lagged correlations suggest a distinct pattern in the variability of Gulf Stream transport and position up- and down-stream of the separation location. However, the correlations cannot identify the forcing mechanisms that ultimately cause the coherent transport anomalies along the SAB and in the Florida Straits and the eventual position anomalies downstream of the separation location. The coherent response along the SAB could reflect the separate responses at different latitudes to changes in the wind field (integrated over characteristics from the North Atlantic interior to the western boundary) that are coherent over large spatial scale. Alternatively, the zero-lag correlations of Florida Current transport with SSH along the SAB could reflect a fast barotropic response to forcing near Cape Hatteras, with the signal propagating equatorward along constant potential vorticity contours (i.e., with the coast on the right). Indeed, one hint that the source of the forcing that drives these spatially coherent transport anomalies may originate in the region near Cape Hatteras comes from P1, the CPIES which was deployed at the 1800-m isobath onshore of the separated Gulf Stream adjacent to the MAB shelf. The lagged correlation between D_T at P1 and Florida Current transport is the highest observed in the cross comparisons made here, with $r = 0.56$ such that D_T at P1 leads Florida Current transport anomalies by 45 days (Figure 11c, blue curve). Detailed interpretation of this signal that leads transport anomalies is beyond the scope of the present study, which focuses on the 19-month PEACH experiment period. It remains to be explored further in future work using the longer time series afforded by wind stress curl reanalysis products, satellite SSH (along-track and mapped), tide gauge records spanning Cape Hatteras, and the Florida Current time series.

The observations from the PEACH CPIESs confirm that Cape Hatteras is a complicated region and that the nature of variability in Gulf Stream position and transport changes markedly where the Gulf Stream transitions from an attached western boundary current to a boundary current extension. Not only does the Gulf Stream interact with the adjacent MAB and SAB shelves here, thereby linking Gulf Stream variability to processes that drive cross-shelf exchange, but Cape Hatteras is also where the Gulf Stream crosses over the Deep Western Boundary Current (Andres et al., 2018), thereby potentially linking local Gulf Stream variability to changes in the basin-wide Atlantic Meridional Overturning Circulation. Gulf Stream separation has proven difficult to model properly (e.g., Chassignet & Marshall, 2008; Saba et al., 2015), and in situ measurements are needed to verify that models are capturing the relevant processes. Future analysis of the PEACH CPIES records will examine the upper-ocean variability (as inferred from the acoustic travel time records and SSH) in the context of the deep variability captured by the CPIESs' bottom pressure and temperature sensors and near-bottom current sensors during the 19-month experiment.

Data Availability Statement

Processed PEACH CPIES data (Andres, 2021) used for the analyses are permanently archived and available at: http://doi.org/10.5281/zenodo.4793504. Spray glider observations used here are available from http://spraydata.ucsd.edu (Todd, 2020b; Todd & Owens, 2016). Satellite data used here are available from Copernicus Marine Service and include along-track data from the global ocean level-3 reprocessed SSH products (SEALEVEL_GLO_PHY_L3_REP _OBSERVATIONS_008_062) and mapped data from the level-4 reprocessed observations (SEALEVEL_GLO_L4_REP_OBSERVATIONS_ 008_047). The Florida Current data are made freely available on the Atlantic Oceanographic and Meteorological Laboratory web page (www.aoml.noaa.gov/phod/floridacurrent/).

Acknowledgments
This research was supported by the National Science Foundation through grant OCE-1558521. Successful CPIES deployments and recoveries were made possible by the skillful efforts of Captain D. Bergeron and the *R/V Neil Armstrong* Crew on cruises AR-15 and AR-33 and is gratefully acknowledged. John Bane's insightful comments on an earlier version of the manuscript are much appreciated, as is the help of Robert Todd and Joleen Heiderich in pulling together the Spray glider data used in this study. Helpful comments from two reviewers are gratefully acknowledged.

References

Andres, M. (2016). On the recent destabilization of the Gulf Stream path downstream of Cape Hatteras. *Geophysical Research Letters*, *43*(18), 9836–9842. https://doi.org/10.1002/2016gl069966

Andres, M. (2020). *Processes driving exchange at Cape Hatteras (PEACH) PIESs and AP technical report – Part 1*. Zenodo. https://doi.org/10.5281/zenodo.4793402

Andres, M. (2021). *Processes driving exchange at Cape Hatteras (PEACH) current- and pressure-sensor equipped inverted-echo-sounder (CPIES) processed datasets [Data set]*. Zenodo. https://doi.org/10.5281/zenodo.4793504

Andres, M., Donohue, K. A., & Toole, J. M. (2020). The Gulf Stream's path and time-averaged velocity structure and transport at 68.5°W and 70.3W. *Deep Sea Research Part I: Oceanographic Research Papers*, *156*, 103179. https://doi.org/10.1016/j.dsr.2019.103179

Andres, M., Muglia, M., Bahr, F., & Bane, J. (2018). On the upper Labrador Sea water at Cape Hatteras. *Scientific Reports*, *4494*. https://doi.org/10.1038/s41598-018-22758-z

Archer, M. R., Shay, L. K., & Johns, W. E. (2017). The surface velocity structure of the Florida Current in a jet coordinate frame. *Journal of Geophysical Research: Oceans*, *122*, 9189–9208. https://doi.org/10.1002/2017JC013286

Bane, J. M., & Brooks, D. A. (1979). Gulf Stream meanders along the continental margin from the Florida Straits to Cape Hatteras. *Geophysical Research Letters*, *6*(4), 280–282. https://doi.org/10.1029/gl006i004p00280

Bane, J. M., Brown, O. B., Evans, R. H., & Hamilton, P. (1988). Gulf Stream remote forcing of shelfbreak currents in the Mid-Atlantic Bight. *Geophysical Research Letters*, *15*(5), 405–407. https://doi.org/10.1029/gl015i005p00405

Bane, J. M., & Dewar, W. K. (1988). Gulf Stream bimodality and variability downstream of the Charleston Bump. *Journal of Geophysical Research*, *93*(C6), 6695–6710. https://doi.org/10.1029/jc093ic06p06695

Chassignet, E., & Marshall, D. (2008). Gulf Stream separation in numerical ocean models. In M. Hecht, & H. Hasumi (Eds.), *Ocean modeling in an eddying regime*. Washington, D.C: American Geophysical Union. https://doi.org/10.1029/177gm05

Cornillon, P. (1986). The effect of the New England Seamounts on Gulf Stream meandering as observed from satellite IR imagery. *Journal of Physical Oceanography*, *16*, 386–389. https://doi.org/10.1175/1520-0485(1986)016<0386:teotne>2.0.co;2

Emery, W. J., & Thomson, R. E. (2004). *Data analysis methods in physical oceanography, second and revised edition* (p. 638). Elsevier.

Fuglister, F. C., & Voorhis, A. D. (1965). A new method of tracking the Gulf Stream. *Limnology & Oceanography*, *10*, 115–124. https://doi.org/10.4319/lo.1965.10.suppl2.r115y7

Glenn, S. M., & Ebbesmeyer, C. C. (1994). Observations of Gulf Stream frontal eddies in the vicinity of Cape Hatteras. *Journal of Geophysical Research*, *99*(C3), 5047–5055. https://doi.org/10.1029/93jc02787

Gula, J., Molemaker, M., & McWilliams, J. C. (2015). Gulf Stream dynamics along the Southeastern U.S. Seaboard. *Journal of Physical Oceanography*, *45*(3), 690–715. https://doi.org/10.1175/jpo-d-14-0154.1

Gula, J., Molemaker, M., & McWilliams, J. C. (2016). Submesoscale dynamics of a Gulf Stream frontal eddy in the South Atlantic Bight. *Journal of Physical Oceanography*, *46*, 305–325. https://doi.org/10.1175/jpo-d-14-0258.1

Haines, S., Seim, H., & Muglia, M. (2017). Implementing quality control of high-frequency radar estimates and application to Gulf Stream surface currents. *Journal of Atmospheric and Oceanic Technology*, *34*(6), 1207–1224. https://doi.org/10.1175/jtech-d-16-0203.1

Halkin, D., & Rossby, T. (1985). The structure and transport of the Gulf Stream at 73°W. *Journal of Physical Oceanography*, *15*, 1439–1452. https://doi.org/10.1175/1520-0485(1985)015<1439:TSATOT>2.0.CO;2

Hall, M. M., & Bryden, H. L. (1985). Profiling the Gulf Stream with a current meter mooring. *Geophysical Research Letters*, *12*, 203–206. https://doi.org/10.1029/gl012i004p00203

Han, L., Seim, H., Bane, J., Todd, R., & Muglia, M. (2021). A shelf water cascading event near Cape Hatteras. *Journal of Physical Oceanography*, *51*, 2021–2033. https://doi.org/10.1175/JPO-D-20-0156.1

Heiderich, J., & Todd, R. E. (2020). Along-stream evolution of Gulf Stream volume transport. *Journal of Physical Oceanography*, *50*(8), 2251–2270. https://doi.org/10.1175/JPO-D-19-0303.1

Johns, W. E., Shay, T. J., Bane, J. M., & Watts, D. R. (1995). Gulf Stream structure, transport and recirculation near 68°W. *Journal of Geophysical Research: Oceans*, *100*(C1), 817–838. https://doi.org/10.1029/94jc02497

Kennelly, M. A., Tracey, K. L., & Watts, D. R. (2007). *Inverted echo sounder data processing manual, GSO technical report. 2007-02*. https://doi.org/10.21236/ada477328

Leben, R. (2005). Altimeter-derived Loop Current metrics. In W. Sturges, & A. Lugo-Fernández (Eds.), *Circulation in the Gulf of Mexico: Observations and models* (pp. 181–202). Washington, D.C.: American Geophysical Union.

Lee, T., & Cornillon, P. (1996). Propagation of Gulf Stream Meanders between 74° and 70°W. *Journal of Physical Oceanography*, *26*(2), 205–224. https://doi.org/10.1175/1520-0485(1996)026<0205:POGSMB>2.0.CO;2

Lee, T. N., Yoder, J. A., & Atkinson, L. P. (1991). Gulf Stream frontal eddy influence on productivity of the southeast U.S. continental shelf. *Journal of Geophysical Research*, *96*(C12), 22191–22205. https://doi.org/10.1029/91jc02450

Lillibridge, J. L., III, & Mariano, A. J. (2013). A statistical analysis of Gulf Stream variability from 18+ years of altimetry data. *Deep Sea Research Part II: Topical Studies in Oceanography*, *85*, 127–146. https://doi.org/10.1016/j.dsr2.2012.07.034

Meinen, C. S., Baringer, M. O., & Garcia, R. F. (2010). Florida Current transport variability: An analysis of annual and longer-period signals. *Deep-Sea Research I*, *57*, 835–846. https://doi.org/10.1016/j.dsr.2010.04.001

Miller, J. L. (1994). Fluctuations of Gulf Stream frontal position between Cape Hatteras and the Straits of Florida. *Journal of Geophysical Research*, *99*(C3), 5057–5064. https://doi.org/10.1029/93jc03484

Miller, J. L., & Lee, T. N. (1995a). Gulf Stream meanders in the South Atlantic Bight 1. Scaling and energetics. *Journal of Geophysical Research*, *100*(C4), 6687–6704. https://doi.org/10.1029/94jc02542

Miller, J. L., & Lee, T. N. (1995b). Gulf Stream meanders in the South Atlantic Bight 2. Momentum Balances. *Journal of Geophysical Research*, *100*(C4), 6705–6723. https://doi.org/10.1029/94jc02541

Muglia, M., Seim, H., & Taylor, P. (2020). Gulf Stream marine hydrokinetic energy off Cape Hatteras, North Carolina. *Marine Technology Society Journal*, *54*(6), 24–36. https://doi.org/10.4031/MTSJ.54.6.4

Saba, V. S., Griffies, S. M., Anderson, W. G., Winton, M., Michael, A., Alexander, M. A., et al. (2015). Enhanced warming of the Northwest Atlantic Ocean under climate change. *Journal of Geophysical Research: Oceans*, *120*. https://doi.org/10.1002/2015JC011346

Sanchez-Franks, A., Flagg, C. N., & Rossby, T. (2014). A comparison of transport and position between the Gulf Stream east of Cape Hatteras and the Florida Current. *Journal of Marine Research*, *72*, 291–306. https://doi.org/10.1357/002224014815460641

Savidge, D. K. (2004). Gulf Stream meander propagation past Cape Hatteras. *Journal of Physical Oceanography*, *34*, 2073–2085. https://doi.org/10.1175/1520-0485(2004)034<2073:gsmppc>2.0.co;2

Savidge, D. K., & Austin, J. A. (2007). The Hatteras Front: August 2004 velocity and density structure. *Journal of Geophysical Research*, *112*, C07006. https://doi.org/10.1029/2006JC003933

Savidge, D. K., & Bane, J. M. (2001). Wind and Gulf Stream influences on along-shelf transport and off-shelf export at Cape Hatteras, North Carolina. *Journal of Geophysical Research*, *106*(C6), 11505–11507. https://doi.org/10.1029/2000jc000574

Thompson, R. O. R. Y. (1979). Coherence significance levels. *Journal of the Atmospheric Sciences*, *36*, 2020–2021. https://doi.org/10.1175/1520-0469(1979)036<2020:csl>2.0.co;2

Todd, R., & Owens, B. (2016). *Gliders in the Gulf stream [data set]*. Scripps Institution of Oceanography, Instrument Development Group. https://doi.org/10.21238/S8SPRAY2675

Todd, R. E. (2020a). Export of Middle Atlantic Bight shelf waters near Cape Hatteras from two years of underwater glider observations. *Journal of Geophysical Research*, *125*, e2019JC016006. https://doi.org/10.1029/2019JC016006

Todd, R. E. (2020b). *Spray glider observations in support of PEACH [Data set]*. Scripps Institution of Oceanography, Instrument Development Group. https://doi.org/10.21238/S8SPRAY0880

Tracey, K. L., & Watts, D. R. (1986). On the Gulf Stream meander characteristics near Cape Hatteras. *Journal of Geophysical Research*, *91*(C1), 7587–7602. https://doi.org/10.1029/jc091ic06p07587

Watts, D. R., & Johns, W. (1982). Gulf Stream meanders: Observations on propagation and growth. *Journal of Geophysical Research*, *87*, 9467–9476. https://doi.org/10.1029/jc087ic12p09467

Watts, D. R., Tracey, K. L., Bane, J. M., & Shay, T. J. (1995). Gulf Stream path and thermocline structure near 74°W and 68°W. *Journal of Geophysical Research*, *100*, 18291–18312. https://doi.org/10.1029/95JC01850